On the other hand, the bimolecular decomposition of acetaldehyde is less influenced by hydrogen, and in a different way.

Increasing pressures of hydrogen rapidly bring the propionic aldehyde reaction to a limiting rate, which is the same as the rate reached when the partial pressure of the aldehyde itself is increased. Similar pressures of hydrogen have no tendency to make the acetaldehyde decomposition appear unimolecular, and no saturation value is reached.

These phenomena are shown to be consistent with the conclusion already reached that the activation of acetaldehyde involves a few degrees of freedom only, while that of propionic aldehyde is a more complex process; and that in the acetaldehyde reaction there is no time-lag between activation and transformation, while in the propionic aldehyde reaction such a time-lag exists.

On the Flow of Air behind an Inclined Flat Plate of Infinite Span.

By A. Fage, A.R.C.Sc., and F. C. Johansen, B.Sc., of the Aerodynamics Department, the National Physical Laboratory.

(Communicated by H. Lamb, F.R.S.—Received May 23, 1927.)

[Plates 6–8.]

§ 1. *Introduction.*

The general form of the flow behind an infinitely long thin flat plate inclined at a large angle to a fluid stream of infinite extent has been known for many years past. The essential features of the motion are illustrated in the smoke photograph given in fig. 1, Plate 6. At the edges, thin bands of vorticity are generated, which separate the freely-moving fluid from the "dead-water" region at the back of the plate; and at some distance behind, these vortex bands on account of their lack of stability roll up and form what is now commonly known as a vortex street* (see fig. 2). Various theories for calculating the resistance of the plate have also been advanced from time to time. One of the earliest is the theory of "discontinuous" motion due to Kirchhoff† and Rayleigh,‡ who

* Bénard, 'Comptes Rendus,' vol. 147 (1876); also Kármán, 'Göttinger Nachr.' (1911 and 1912).

† 'Crelle,' vol. 70 (1869).

‡ "Notes on Hydrodynamics," 'Phil. Mag.' (1876).

obtained the expression $\frac{\pi \sin \alpha}{4 + \pi \sin \alpha} \rho V_0^2 b$ (see symbols) for the normal force per unit length of the plate. More recently Kármán* has obtained a formula for the resistance of a plate normal to the general flow, in terms of

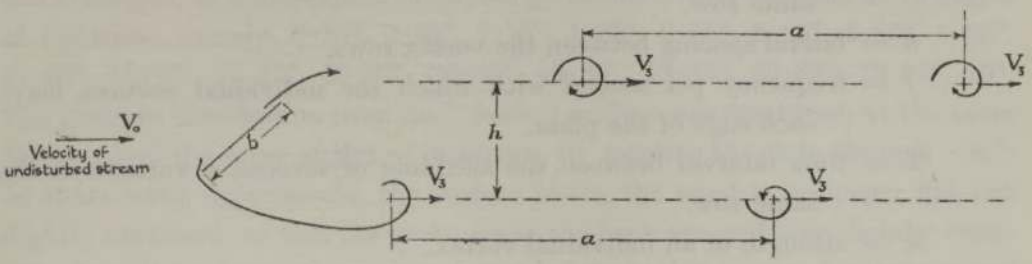

FIG. 2.

the dimensions of the vortex system at some distance behind the plate. In spite, however, of these and other important investigations, much more remains to be discovered before it can be said that the phenomenon of the flow is completely understood.

No attempt has hitherto been made, as far as the writers are aware, to determine experimentally, at incidences below 90°, the frequency and speed with which the vortices pass downstream; the dimensions of the vortex system; the average strength of the individual vortices; or the rate at which vorticity is leaving the edges of the plate. The present investigation† has been undertaken to furnish information on these features of the flow.

§ 2. *List of Symbols.*

V = average velocity at any point in the field.
V_0 = velocity of the undisturbed air relative to the plate.
V_1 & V_2 = velocity in the outer and inner boundaries of the vortex band at the edge of the plate.
V_3 = downstream velocity of the individual vortices ($V_3 = f.a$).
p_0 = pressure in the undisturbed air.
p = pressure at any point of the field.
p_m = mean pressure at the back of the plate.
α = angle of incidence of the plate (degrees).
b = breadth of plate.

* 'Göttinger Nachr.' (1911 and 1912); also Heisenberg, 'Phys. Z.' (1922).

† Permission to communicate the results was kindly granted by the Aeronautical Research Committee.

x, y = the longitudinal and lateral co-ordinates of a point in the field. They are measured from the centre of the plate along and at right angles to the undisturbed wind direction.

a = longitudinal spacing between two consecutive vortices in the same row.

h = lateral spacing between the vortex rows.

f = frequency per second with which the individual vortices leave each edge of the plate.

T = time interval between the shedding of successive vortices in the same row.

κ = strength of an individual vortex.

K = total strength of vorticity leaving each edge in one second.

k_N = normal force coefficient = (normal force per unit length)/$\rho b V_0^2$.

ρ = density of the air.

§ 3. *Forces on the Plate.*

(3.1.) The experiments were made on a flat, sharp-edged rectangular steel plate. The dimensions were: length 7 feet (approximately), and breadth 5·95 inches. The cross-section of the plate, normal to the span, is shown in fig. 3. To obtain the necessary rigidity, one surface (the front) was flat, and

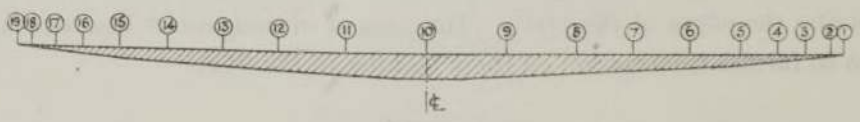

Fig. 3.

the other was slightly tapered from the centre—where the thickness is 3 per cent. of the breadth—towards the sharp edges. The plate was mounted vertically with small clearances between its ends and the floor and roof of one of the 7-foot wind-tunnels at the N.P.L. Observations, whether of pressure on the plate or of velocity in the stream were confined to the plane of symmetry, midway between the floor and roof, where for all practical purposes the flow is two-dimensional.

(3.2.) The forces on the plate inclined at various angles to the wind were estimated, for two-dimensional flow, from observations of pressure taken around the median section. For this purpose, a pressure tube of fine bore, into which 19 small holes were subsequently drilled—the positions are shown in fig. 3—was let in flush with the flat surface. The pressure in this tube was conveyed through a second tube, at right angles to the first and also flush with the surface,

to the pressure manometer, which was a standard 26-inch Chattock tilting gauge. The holes were made airtight by thin paper discs glued to the surface of the plate. To measure the pressure, each hole was opened, in turn, to the air, by the removal of a paper disc. The pressure distribution over the front surface was measured, at a wind speed of 50 feet per second, with the plate at 18 angles of incidence, namely, 0·15°, 0·85°, 1·15°, 1·85°, 2·15°, 3·85°, 5·85°, 8·85°, 11·85°, 14·85°, 19·85°, 29·85°, 39·85°, 49·85°, 59·85°, 69·85°, 79·85°, 90°. The pressure distribution over the " back " surface was measured, at the same holes and at the same angles of incidence, by rotating the plate through 180°. In these latter experiments, the surface facing the wind is no longer flat but slightly cambered, so that the pressures at the back are probably slightly different, at small incidences, from those for an infinitely thin plate. No attempt was made to measure this difference, since a few observations taken with a total-head tube showed that, at large angles of incidence, the pressure in the dead-air region immediately behind the plate was the same, within the accuracy of measurement, whether the flat or slightly cambered surface was presented to the wind.

(3.3.) The values of the normal force coefficient, k_N, were estimated from the areas of the diagrams obtained when the pressure coefficients $(p - p_0)/\rho V^2$ were plotted on a base representing the width of the plate. To illustrate their general character, six representative diagrams are given in fig. 4.

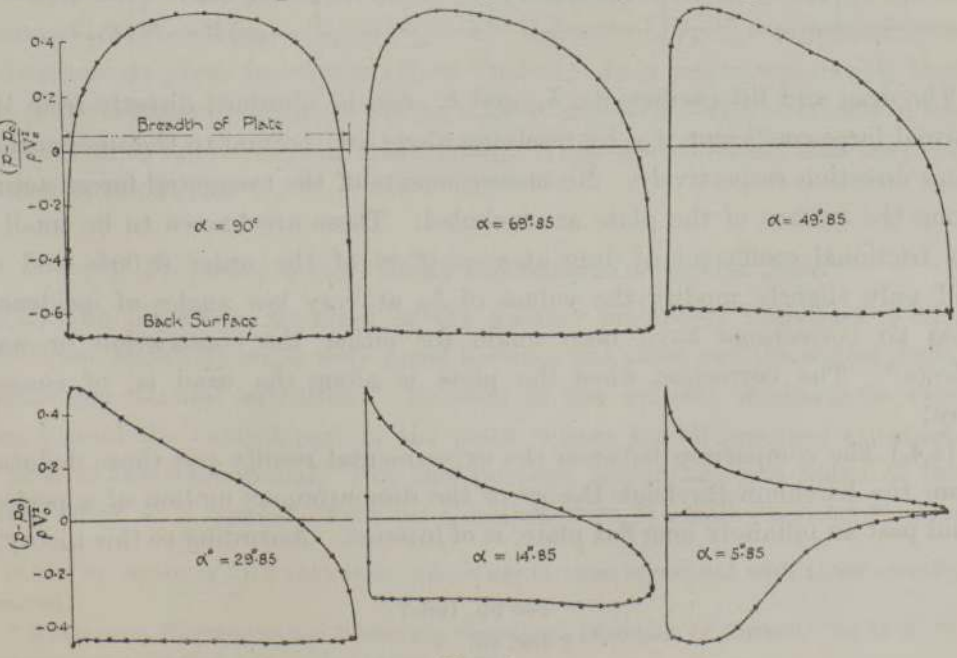

FIG. 4.

The estimated values of k_N are given in Table I (column A). These results show that k_N increases fairly rapidly with α, until a value of 0·445 is reached at $\alpha = 9°$. Beyond this incidence, k_N falls slowly to a value 0·425 at $\alpha = 15°$, and then increases continuously to a maximum value 1·065 at $\alpha = 90°$.

Table I.

$\alpha°$	k_N.			Wind-tunnel values of $(p_m - p_0/\rho V_0^2)$	$(V_1/V_0)^2$.
	Wind tunnel. (A)	Kirchhoff-Rayleigh. (B)	Ratio of wind-tunnel k_N to theoretical k_N. (C)	(D)	(E)
0	0	0	—	—	—
3	0·165	0·040	4·10	—	—
6	0·345	0·075	4·60	—	—
9	0·445	0·110	4·05	—	—
15	0·425	0·170	2·50	—	—
20	0·470	0·215	2·20	—	—
30	0·645	0·280	2·30	−0·462	1·92
40	0·785	0·335	2·35	−0·544	2·09
50	0·900	0·375	2·40	−0·615	2·23
60	0·985	0·405	2·45	−0·664	2·33
70	1·035	0·425	2·45	−0·680	2·36
80	1·060	0·435	2·45	−0·688	2·38
90	1·065	0·440	2·45	−0·690	2·38

The drag and lift coefficients, k_D and k_L, can be obtained directly from the normal force coefficient, k_N, by resolving along and normal to the undisturbed wind direction respectively. No measurements of the tangential forces acting along the surface of the plate are included. These are known to be small—the frictional coefficient of drag at $\alpha = 0°$ is of the order 0·004—and so will only slightly modify the values of k_D at very low angles of incidence. Also no corrections have been made for either the constriction or wall effects.* The correction when the plate is along the wind is, of course, zero.

(3.4.) The comparison between the experimental results and those deduced from the Kirchhoff-Rayleigh theory of the discontinuous motion of a perfect fluid past an infinitely long flat plate, is of interest. According to this theory,†

* See pp. 196–7.

† *Loc. cit.*

the normal force coefficient k_N is equal to $\pi \sin \alpha/(4 + \pi \sin \alpha)$, and is derived on the assumptions (*a*) that the air breaks away from the plate at the sharp edges and leaves a " dead-air " region behind the plate, throughout which the pressure is uniform and equal to that in the undisturbed fluid, and (*b*) that both the pressure and velocity in the free surfaces separating the stationary from the moving fluid are equal to those in the undisturbed fluid. The theoretical values of k_N are given in Table I, together with the experimental results. It is seen that the theory considerably under-estimates the value of k_N over the entire range of incidence.

(3.5.) An explanation of the marked differences between the theoretical and experimental values of k_N may be found in the fact that the maximum velocity (V_1) in the boundary of the dead-air region behind the plate is appreciably greater than the velocity V_0 assumed in the theory, and that the mean pressure p_m behind the plate is, as a consequence, much lower than p_0. At values of α greater than 30°, the experimental pressure p_m at the back of the plate is approximately uniform, and variations from the mean value do not exceed $\pm$ 3 per cent. (see fig. 4). These mean values of $(p_m - p_0)/\rho V_0^2$ are given in column (D) of Table I. If it be assumed that the total head of the air, in the *outer boundary* of the vortex band (*i.e.*, band of discontinuity) leaving an edge of the plate is equal to that in the undisturbed stream, and that the pressure there is equal to that at the back of the plate, the velocity V_1 along this boundary is given by the relation $(V_1/V_0)^2 = 2(p_0 - p_m)/\rho V^2{}_0 + 1$. Values* of $(V_1/V_0)^2$ estimated from this relation are given in column (E) of Table I. It is rather remarkable that they agree very approximately—except at low values of α—with the ratios of the experimental to the theoretical values of k_N. It is for this reason that they are included in the Table.

§ 4. *Frequency of the Velocity Fluctuations behind the Plate.*

(4.1.) The plate was mounted in the manner previously described (§ 3.1). In addition, stiffening wires were fitted between the plate and the tunnel walls, to eliminate flexural vibrations. Records of the velocity fluctuations were taken behind the central part of the plate, where, for all practical purposes, the flow is two-dimensional. For this purpose, advantage was taken of the cooling effect of a current of air on a heated wire of small diameter.† The

* It will be shown in § 6.3 that these values are in close agreement with those actually measured.

† " A Hot-wire Instrument for Measuring Speed and Direction of Airflow," by L. F. G. Simmons and A. Bailey, ' Phil. Mag.' (Jan., 1927).

current fluctuations in the hot wire circuit due to the fluctuations of wind speed, were passed through an Einthoven galvanometer, fitted with lantern and camera, and the displacement of the string photographically recorded. Time spacings of 1/50 second, obtained from a phonic-wheel time marker controlled by a 50 ~ tuning fork, were included in the records.

(4.2.) A sketch of one of the hot wires used is given in fig. 5A. The wire—of platinum 0·001-inch diameter and about 0·3 inch long—was always mounted

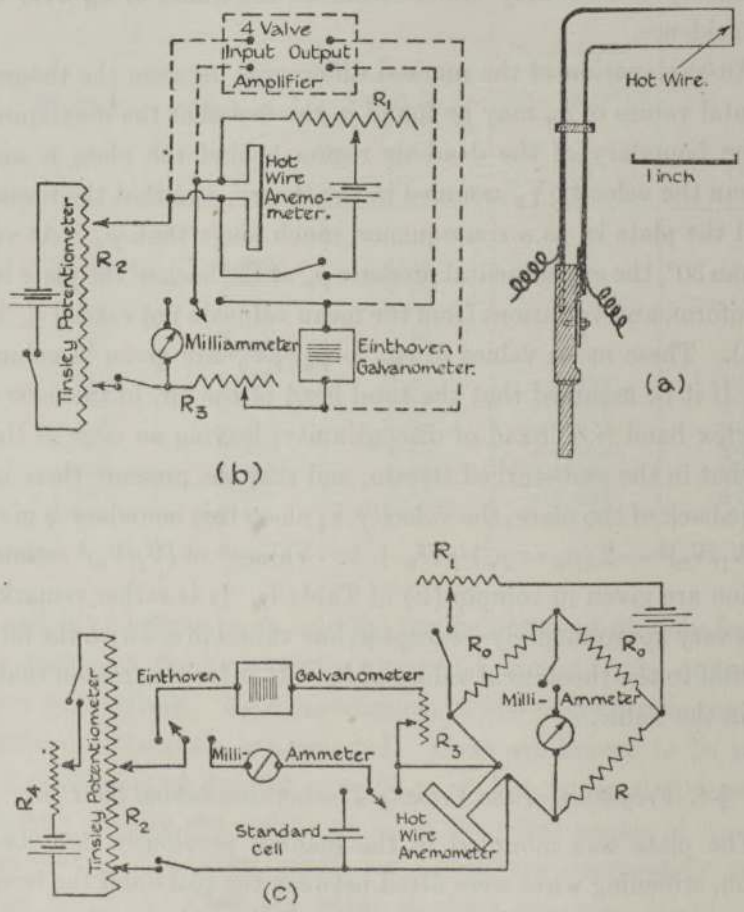

FIG. 5.

parallel to a sharp edge of the plate, that is, normal to the plane of the two-dimensional flow, and was therefore influenced only by changes of wind speed, not by fluctuations of wind direction. The general method of experiment can best be described by reference to the diagram given in fig. 5B. The wire, mounted in the wind stream at the point where the speed fluctuations were to be detected, was heated to a dull red glow by an electric current controlled by the rheostat

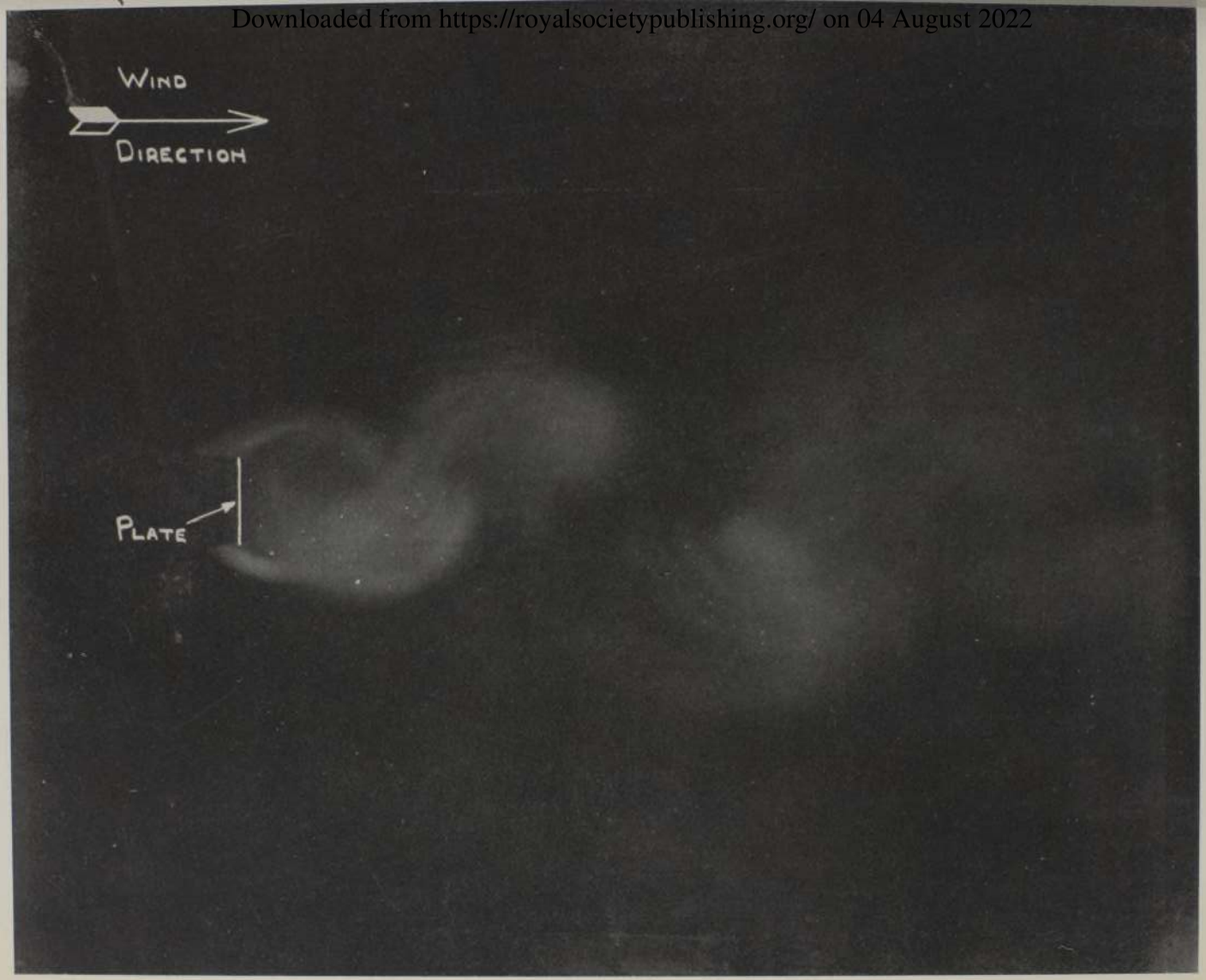

FIG. 1.

(*Facing p.* 176.)

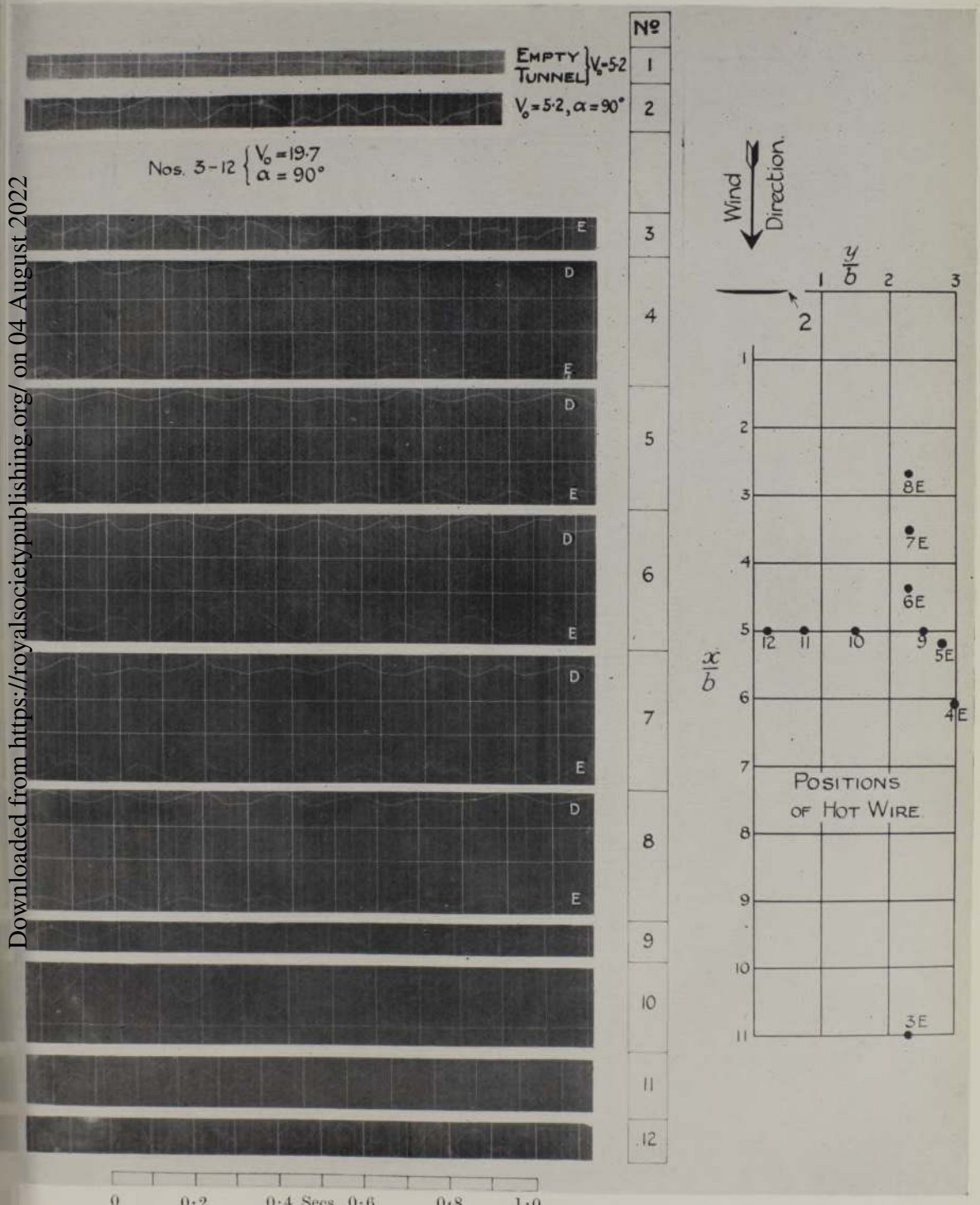

FIG. 6.

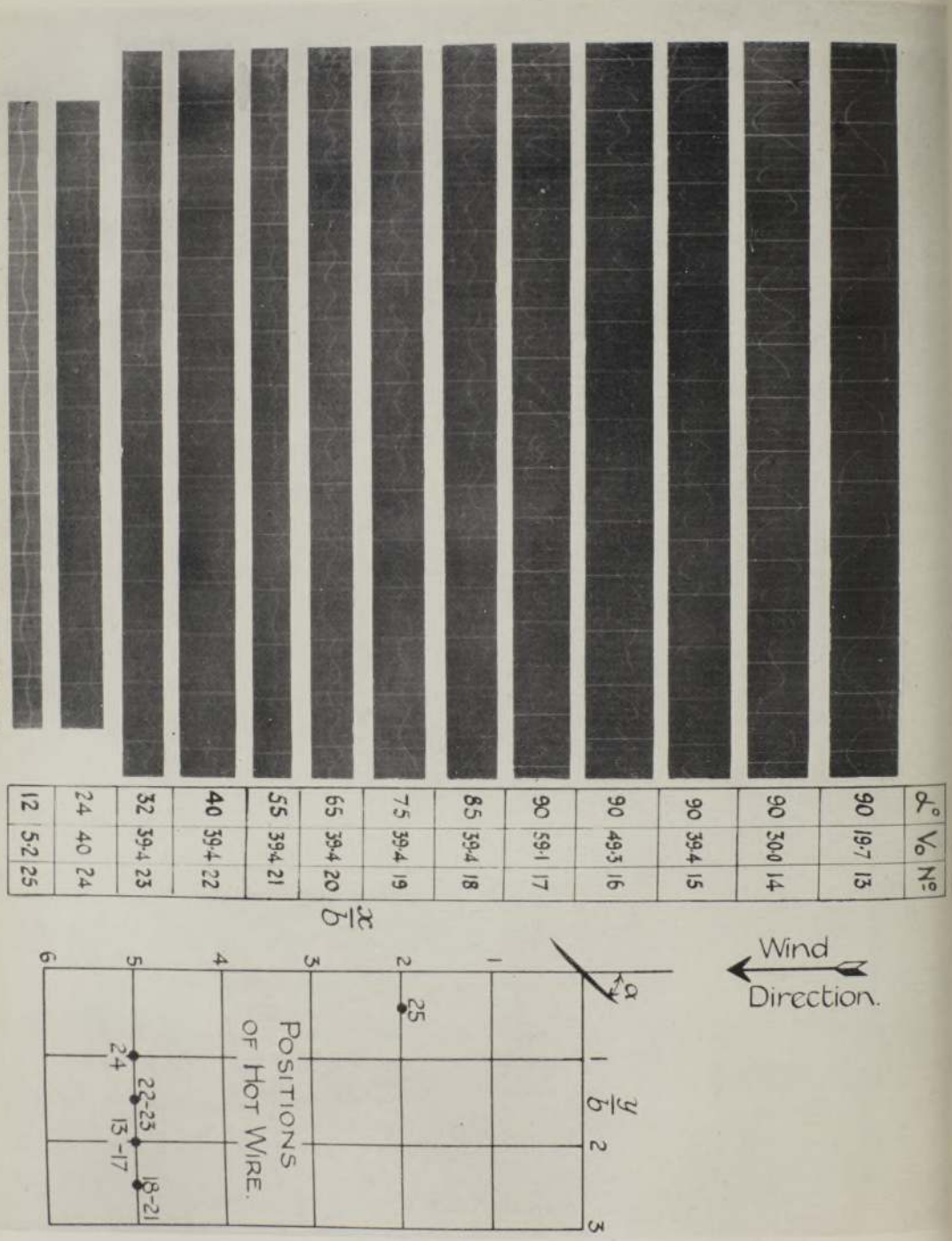

Fig. 7.

R_1. The average potential difference between the ends of the hot wire was then balanced on a potentiometer, a milli-ammeter being used as an indicator. The milli-ammeter was then switched out and the fluctuations in the potential between the ends of the hot wire put directly across the Einthoven galvanometer. A second circuit (shown dotted) containing a four-valve resistance amplifier* was used on a few occasions, when the speed fluctuations were a small proportion of the mean speed. The deflection of the Einthoven string was adjusted either by altering its tension or by a change in the resistance R_3.

(4.3.) At the outset, records of the velocity fluctuations were taken at a large number of positions in the field, with the plate at 90°. The position of a point in the field is given by the co-ordinates x and y, measured from the centre of the plate, respectively along and at right angles to the direction of the undisturbed wind. The positive direction of x is downstream, and that of y to the left when looking downstream (see Plates 7 and 8). The purpose of this exploration was to determine how the general character of the velocity fluctuations varied in different parts of the field, and also to see whether the frequency of these fluctuations was uniform. The records were taken at a low speed (19·7 feet per second) in order that any lag in the response of the hot-wire—this does not, of course, affect the recorded frequency—should not appreciably misrepresent the general character of the velocity fluctuations.

(4.4.) Records (without amplification) were taken along a longitudinal line ($y = 2.3b$) some distance outside the edge of the plate; across the wake along the line $x = 5b$; at the edge; and also in front of the plate. A representative selection of these Einthoven records is photographically reproduced in Plate 7. Records of the disturbance in the empty tunnel were also taken. In these early experiments no attempt was made to measure the actual magnitude of the velocity fluctuations. Their relative magnitudes are, however, conveyed with sufficient accuracy in the diagrams. The points of interest which arise from the records in fig. 6 (Plate 7) ($\alpha = 90°$) are summarised below. For convenience of reference the records are numbered; also a diagram is attached giving the positions of the hot wire.

(*a*) The velocity fluctuations in the empty tunnel (No. 1) are very small compared with those at the back of the plate (Nos. 3 to 12). It will be shown later that this was the case not only at 90° but at all angles of incidence greater than 12°.

* A comparison of diagrams taken with and without amplification, showed that the amplifier did not introduce any apparent extraneous frequencies.

(*b*) The velocity fluctuations at the edge of the plate are large but do not appear to be very regular (No. 2).

(*c*) There is a region, outside the wake and at some distance behind the plate, where the velocity fluctuations are very regular (Nos. 5 to 8), also (Nos. 13 to 17).

(*d*) The velocity fluctuations tend to become less regular as the distance behind the plate increases beyond $3b$ (Nos. 3E to 8E).

(*e*) The velocity fluctuations within the wake are more irregular than those outside (Nos. 9 to 12).

(*f*) At the same wind speed, the frequency of the fluctuations at all points behind the plate, and at some distance outside what were later decided to be the limits of the vortex street, is uniform (Nos. 4 to 8).

(*g*) The frequency of the fluctuations at the centre of the vortex street is, in general, double that outside (Nos. 9 and 12).

In addition, it was found that the velocity fluctuations at some distance forward of the plate ($4b$) were very small compared with those at the back; and also that the fluctuations in the plane of the plate and at some distance from the edge were small and irregular. It should also be noted that the amplitude of the fluctuations at $y = 1{\cdot}52b$ (No. 10) is greater than those on either side (Nos. 9 and 11). This is of interest because, as will be shown later, the limit of the wake is situated near the line, $y/b = 1{\cdot}5$.

(4.5.) The most important conclusion which may be drawn from the above summary of results is that there is a large region situated outside the wake, and at some distance behind the plate, where well-defined fluctuations of velocity of uniform frequency can be clearly determined. The photograph* of fig. 1, and also the work of previous investigators, leaves no room for doubt that these fluctuations are caused by the passage downstream of large vortices. The records demonstrate therefore that these vortices are shed from each edge of the plate with uniform frequency; and also that the frequency with which these individual vortices are generated can best be measured at some distance outside the vortex street, where the fluctuations are comparatively steady. For brevity, the frequency with which the vortices leave the edges of the plate will be referred to hereinafter as the "frequency." The variation of the magnitude of the velocity fluctuation, at any point in the field, is considered later.

(4.6.) Several records were taken to show how the frequency varied with wind

* The "smoke" was obtained by mixing ammonia and hydrochloric acid in front of the plate.

speed, at a constant angle of incidence (90°). Some of these records are given in Plate 8 (Nos. 13 to 17), in order to show the regularity with which the fluctuations of velocity occur. Values of "f" estimated from records of this character are collected in Table II. The last column of this table shows that from $V_0 = 10$ to $V_0 = 60$ feet per second, the frequency is directly proportional to speed, within the accuracy of observation.

Table II.—$\alpha = 90°$.

V_0.	f.	fb/V_0.
10·6	3·13	0·146
19·7	5·75	0·144
30·05	9·00	0·148
39·40	11·60	0·146
49·25	14·55	0·146
59·10	17·35	0·146

(4.7.) A large number of records was taken to show the variation of frequency with the inclination of the plate. A representative selection of these records for values of α betwen 12° and 90° is given in Plate 8 (Nos. 17 to 25). They show that the velocity fluctuations are fairly regular, the best diagrams being obtained at high angles of incidence. The velocity fluctuations at the lowest angle of incidence (12°) are, it should be observed, much larger and easily distinguishable from the velocity disturbances in the empty tunnel (Nos. 1 and 25). The values of the frequency, estimated from these and similar records and expressed in the non-dimensional form (fb/V_0), are collected in Table III.

Table III.

α°.	fb/V_0.	$fb \sin \alpha/V_0$.	α°.	fb/V_0.	$fb \sin \alpha/V_0$.
90	0·146	0·146	24	0·394	0·160
85	0·147	0·146	20	0·478	0·164
80	0·152	0·150		0·503	0·172
75	0·153	0·148	16	0·548	0·151
70	0·156	0·147		0·677	0·187
65	0·163	0·148	14	0·746	0·181
60	0·173	0·150		0·900	0·218
55	0·182	0·149	12	0·874	0·182
50	0·196	0·150		0·880	0·183
45	0·205	0·145			
40	0·231	0·148	70	0·156	0·146
36	0·253	0·149	60	0·171	0·148
32	0·280	0·148	* 50	0·193	0·148
30	0·307	0·153	40	0·233	0·150
28	0·330	0·155	30	0.304	0·152

* These observations were taken on the opposite side of the wake to that for the earlier results.

At several angles of incidence, two observations were taken, one on each side of the vortex street. In each case, the two values were in close agreement and this indicates that the vortices are shed from each edge with the same frequency. The table shows that the frequency increases, at first slowly and then more rapidly, as the angle of incidence decreases progressively from 90°. It will also be observed that $fb \sin \alpha / V_0$ is approximately constant and equal to 0·148 for values of α between 90° and 30°.

(4.8.) Records of the velocity disturbances (with and without amplification) were also taken with the plate at incidences below 12°. The results of this work are not included in the paper because the disturbances were not sufficiently regular to allow a reliable estimate of the frequency to be made. This was largely because (at low incidences) the disturbances in the region of the plate were of the same character as those in the wind of the empty tunnel. There is, however, some evidence—based on work done on the standard plate and also on another plate, 2·3 times as wide—to show that between 0° and 9° the values of (fb/V_0) probably lie somewhere between 1·0 and 1·6.

§ 5. *Longitudinal Spacing of Vortices.*

(5.1.) The method of measurement is based on the fact that the velocity fluctuations at two points situated without, and on the same side of, the vortex street are in phase, when the longitudinal distance between the points is equal to the distance between successive vortices in the same row, or a multiple of this distance. To determine the phase difference between two points, two hot wires were used and simultaneous records of the velocity disturbances taken. The average time displacement between the two series of crests (or troughs) expressed as a fraction (t/T) of the periodic time gave the phase difference.

In practice, one hot wire was fixed, and the other, usually on the opposite side of the vortex street, was moved up and down stream along a line outside the vortex street. Representative diagrams, taken with the plate at 90° incidence and the datum hot wire (D) at the position $x/b = 6{\cdot}0$, $y/b = -3{\cdot}0$, are given in Plate 7 (Nos. 4 to 8). Record No. 4 shows that when the hot wires are situated at the same distance behind the plate, but on opposite sides of the vortex street, the velocity fluctuations are 180° $(t/T = 0{\cdot}5)$ out of phase.

(5.2.) The values in Table IV give, for various angles of incidence, the variation of phase difference (t/T) with the distance downstream. At each angle of incidence, these observations plot fairly smoothly on a straight line. The longitudinal spacing (a) between consecutive vortices in the same row—that is,

the change in the value of x for unit phase difference—was obtained directly from these lines.

Table IV.—Values of (t/T).

x/b.	$\alpha = 90°$.	$\alpha = 70°$.	$\alpha = 60°$.	$\alpha = 50°$.	$\alpha = 40°$.	$\alpha = 30°$.
2·02	−0·12	−0·10	−0·23	−0·21	−0·40	−0·58
3·02	+0·07	+0·10	0	−0·01	−0·16	−0·13
4·03	0·31	0·34	+0·24	+0·24	+0·13	+0·20
5·04	0·50	0·50	0·45	0·51	0·42	0·43
6·05	0·64	0·73	0·70	0·76	0·72	0·90
7·06	0·83	0·92	0·93	1·01	1·04	1·24
8·06	1·05	1·13	1·15	1·24	1·31	1·55
9·07	1·24	1·29	1·37	1·48	1·49	1·90
10·08	1·41	1·55	—	1·71	1·81	2·31
11·09	1·62	1·71	—	—	—	—
12·10	1·78	—	—	—	—	—

Table V.

$\alpha°$	(a/b)	$(a/b \sin \alpha)$	$(V_3/V_0 = af/V_0)$
90	5·25	5·25	0·766
70	4·85	5·17	0·756
60	4·44	5·13	0·761
50	4·08	5·33	0·789
40	3·55	5·52	0·817
30	2·76	5·52	0·840

The estimated values of (a/b) are given in Table V. The longitudinal spacing is seen to decrease as the angle of incidence of the plate decreases. It will also be noted that, for values of α between 30° and 90°, the value of $(a/b \sin \alpha)$ is approximately constant, that is, the longitudinal spacing is proportional to $(b \sin \alpha)$.

(5.3.) The last column of Table V gives the ratio of the speed with which the vortices pass downstream (V_3) to the velocity of the undisturbed wind (V_0). Each value of V_3 was directly obtained from the product of "a" and "f," for, in unit time, "f" vortices spaced a distance "a" apart pass downstream. It is seen that the value of V_3/V_0 progressively increases from 0·766 at $\alpha = 90°$ to 0·840 at $\alpha = 30°$.

§ 6. *Velocity and Vorticity at the Edge of the Plate.*

(6.1.) The experiments described in this section of the paper were made to measure, at several angles of incidence, the velocity distribution near the edge of the plate. The purpose of these experiments was two-fold: to make a

comparison between the velocity actually measured at the edge and that estimated from the measured pressure immediately behind the plate; and to estimate the rate at which vorticity is shed from each edge.

Two series of velocity measurements were made. In the first, Series A, the exploration was made at several angles of incidence, across the boundaries of the dead-air region, along a line normal to the edge and the undisturbed wind direction at a distance of $0{\cdot}033b$ behind each edge of the plate. Explorations were also made for $\alpha = 90°$ at distances $0{\cdot}084b$ and $0{\cdot}168b$ behind the plate. In the second series (B), the measurements were made in the plane of the plate outwards from each edge. In each series, the hot wire was mounted parallel to the edge and the time average of the velocity at a point was measured. The method of measurement is illustrated in fig. 5c (excluding Einthoven galvanometer circuit). The hot wire formed one arm of a Wheatstone Bridge, and its mean resistance (and therefore its temperature) was maintained constant at all speeds by an adjustment of the resistance R_1. The potential difference between the ends of the hot wire, measured on a potentiometer, is then a function of the *mean* wind speed at the point. The calibration curve was obtained, before and after each set of observations, by mounting the hot wire in the empty tunnel and recording changes of potential difference as the wind speed was progressively changed. The E.M.F. across the potentiometer was maintained at a constant value by adjusting the resistance R_4, so that the drop of potential along a fixed length of the potentiometer wire just balanced the constant E.M.F. of a standard cell.

(6.2.) The velocity was measured at both the leading and trailing edges, at $\alpha = 90°$, 70°, 50° and 30° respectively. The observations are plotted in figs. 8 and 9. These curves show very clearly the rapid increase of velocity across the dead-air boundary at each edge of the plate. The narrow band over which the rapid change of velocity occurs will hereinafter be called the " vortex band." The more important results in figs. 8 and 9 have been collected in Table VI. From these results it is evident that:

(*a*) The velocity V_1—that is, the velocity in the outer boundary of the vortex band—measured in the plane of the plate (Series B) is in close agreement, at both the leading and trailing edges, with that measured about $0{\cdot}033b$ behind the edge (Series A). Columns (*a*) to (*e*).

(*b*) The values of (V_1/V_0) at both the leading and trailing edges decrease as α decreases. Columns (*a*) to (*e*).

(*c*) At each angle of incidence, the values of (V_1/V_0) at the leading and trailing edges are in close agreement. Columns (*a*) to (*e*).

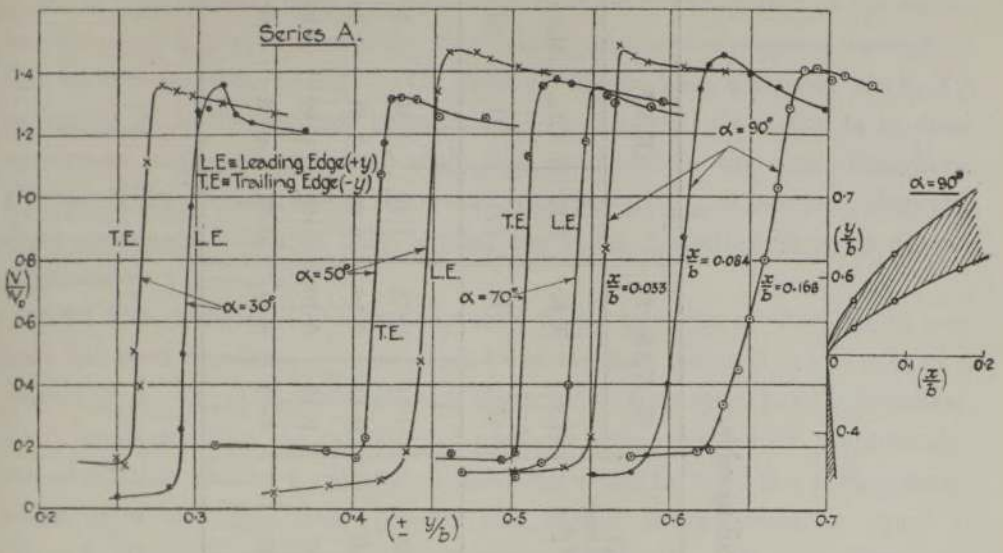

FIG. 8.

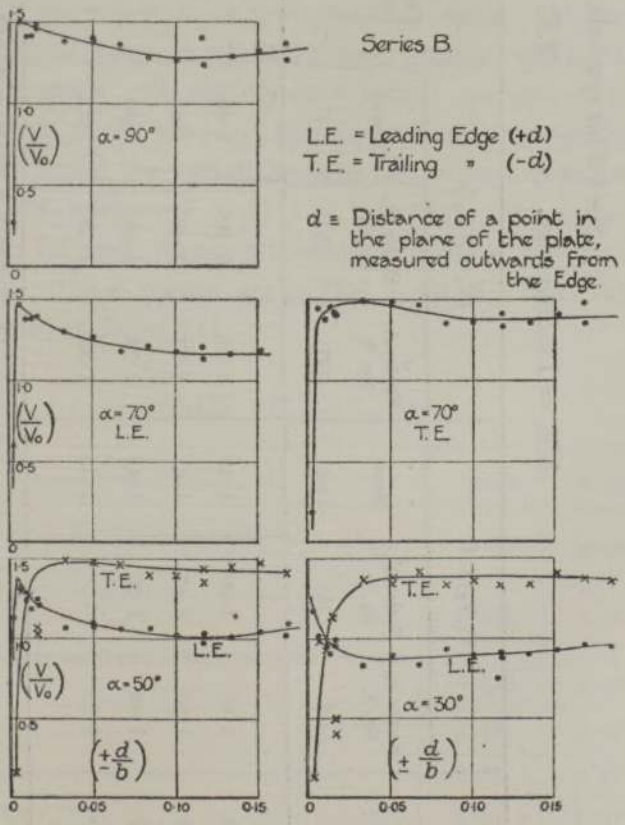

FIG. 9.

Table VI.

See § 2 for symbols.

L.E. = Leading edge. T.E. = Trailing edge.

α°	(V_1/V_0) L.E.			(V_1/V_0) T.E.			(V_1/V_0) Estimated from measured p_m.	(V_2/V_0) fig. 8.		(K/V_0^2).		
	Series A, fig. 8. (*a*)	Series B, fig. 9. (*b*)	Mean. (*c*)	Series A, fig. 8. (*d*)	Series B, fig. 9. (*e*)	Mean. (*f*)	(*g*)	L.E. (*h*)	T.E. (*i*)	L.E. (*j*)	T.E. (*k*)	Mean. (*l*)
90	1·48	1·50	1·49	1·48	1·50	1·49	1·545	0·14	0·14	1·10	1·10	1·10
70	1·35	1·47	1·41	1·37	1·48	1·43	1·540	0·14	0·16	0·99	1·01	1·00
50	1·46	1·37	1·42	1·32	1·48	1·40	1·495	0·10	0·16	1·00	0·97	0·99
30	1·35	—	1·35	1·36	1·38	1·37	1·385	0·07	0·14	0·91	0·93	0·92

* $(V_1/V_0)^2 = 1 + 2\,[(p_0 - p_m)/\rho V_0^2]$.

(*d*) If it be assumed that the total head in the outer boundary of the vortex band is equal to that in the undisturbed wind, and that the pressure throughout this band is the same as that in the dead-air region, then the value of (V_1/V_0) estimated from the average pressure (p_m) in the dead-air region is in close agreement (within 5 per cent.) with that measured in the outer boundary. Further, if the pressure across the vortex band is uniform, as assumed, then this close agreement indicates that beyond the outer boundary there is a near approach to a potential flow.

(6.3.) The strength of the vorticity shed from each edge of the plate in unit time has been estimated by a method based on that followed in the case of a perfect fluid. On the assumption that the width of the vortex band is infinitesimally small, and that the velocities on opposite sides are V_1 and V_2 respectively, the circulation around a rectangle containing a length δs of the vortex sheet, whose sides are respectively parallel and normal to the sheet, is equal to $(V_1 - V_2)\delta s$, that is $(V_1^2 - V_2^2)\delta t/2$ since $\delta s/\delta t = (V_1 + V_2)/2$. The total amount of vorticity leaving the edge in unit time is therefore $(V_1^2 - V_2^2)/2$ or $(V_1^2 - V_2^2)/2V_0^2$ expressed in non-dimensional units. In the actual flow, however, the vortex hand is of finite and varying width; the radius of curvature also changes with the distance behind the plate. It is necessary, therefore, to determine the shape of the vortex band at some distance behind the edge to see whether the vortex strength can be estimated with reasonable accuracy from the relation $K = (V_1^2 - V_2^2)/2V_0^2$. The vortex band was, therefore, located for some distance behind the plate at $\alpha = 90°$, by explorations of velocity. These results are plotted in fig. 8. Data taken from this figure are tabulated in Table VII.

Table VII.—$\alpha = 90°$.

Distance behind plate (x/b):	0	0·033	0·084	0·168
(y/b) co-ordinate of point of maximum velocity, V_1	0·505	0·570	0·630	0·695
(y/b) co-ordinate of point of minimum velocity, V_2	—	0·535	0·570	0·613
Ratio of width of vortex band to the breadth of the plate	—	0·035	0·060	0·082
Value of (V_1/V_0)	1·50	1·49	1·47	1·42
Value of (V_2/V_0)	—	0·14	0·17	0·18
Value of $(V_1^2 - V_2^2)/2V_0^2$	1·11	1·10	1·07	0·99

The opening-out of the vortex band with increasing distance behind the plate is clearly shown in fig. 8. This figure together with the results in Table VII show that the width of the vortex band, although increasing with the distance downstream, is small compared with the radius of curvature of the centre line of the band, and also that the velocities along both the outer and inner boundaries are uniform, within the accuracy of measurement, for some distance behind the plate. It is concluded, therefore, that the value of $(V_1^2 - V_2^2)/2V_0^2$ measured close behind the plate gives a reasonably accurate approximation to the strength of the vorticity leaving the edge in unit time.

The estimated values of (K/V_0^2) are given in columns (j) and (k) of Table VI. These results show that only a slight diminution in the strength of the vorticity leaving each edge accompanies the considerable decrease in α from 90° to 30°; also that the vorticity is shed from the two edges of the plate at the same rate.

§ 7. *Magnitude of the Velocity Fluctuations behind the Plate.*

(7.1.) The experiments now to be described were made to measure at several angles of incidence, the mean speed and also the magnitude of the velocity fluctuations, at some distance behind the plate. The purpose in view was the determination of the average strength of the individual vortices passing downstream (see § 8). The results themselves also bring to notice some general characteristics of the flow.

The measurement of mean velocity was made by the method described in § 6.1. To measure the amplitude of the fluctuations, the mean potential difference between the ends of the hot wire was balanced on the potentiometer, and then the current fluctuations in the circuit were passed directly through the Einthoven galvanometer (fig. 5) and a record of the motion of the string taken.

To obtain a direct calibration of the string, the hot wire was mounted in the empty tunnel, and the wind speed adjusted until its value (as indicated on the potentiometer) was the same as that of the mean speed obtaining when the records of the velocity fluctuations were taken. The Einthoven galvanometer was then switched into the hot-wire circuit, and records taken of the displacement of the string as the tunnel speed was varied.

(7.2.) Observations of the mean speed and records of the velocity fluctuations were taken both within and outside the vortex street at some distance behind the plate. The distances were $5b$, $10b$ and $20b$ at $\alpha = 90°$, and $8b$ at $\alpha = 70°$ and $\alpha = 40°$. The measurements were made at a low wind speed (about 10

feet per second), to minimise errors of measurement due to any lag in the response of the hot wire to the velocity fluctuations. A comparison of results taken at speeds below and above 10 feet per second showed that if there is an error due to lag, it is smaller than the usual irregularities in the velocity fluctuations at a constant value of V_0; in fact, the records showed—except at some distance outside the limits of the vortex street—that, at any point in the field, there were large variations with time, in the values of both the maximum and minimum velocities. The average magnitude of the velocity fluctuations was estimated, therefore, from the average displacement between a large number of crests and troughs. It was also found, from an analysis of a number of records, that the difference between the average maximum velocity and the mean velocity was about 45 per cent. of the average difference between the maximum and minimum velocities. The maximum velocity has therefore been taken as the sum of the mean velocity (as measured on the potentiometer) and 45 per cent. of the average difference between the maximum and minimum velocities (obtained from the Einthoven records); and the minimum velocity as the mean velocity less 55 per cent. of this average difference. The maximum and minimum velocities could have been determined directly, with the Einthoven galvanometer, but the reason this was not done was because, as will appear later, it was the differences between these values, not their actual magnitudes, that were needed in the determination of the strength of the individual vortices.

(7.3.) The results of these experiments are given in figs. 10 and 11. At $\alpha = 90°$, and for all practical purposes at $\alpha = 70°$, the velocity curves were found to be symmetrical about the centre line of the wake ($y = 0$), so that only the curves for the positive values of y are given. This was not the case at $\alpha = 40°$, so that curves have been drawn for both positive and negative values of y. The points on each curve of maximum and minimum velocity represent mean values taken from two or more records.

It will be observed that each set of curves in figs. 10 and 11 exhibit similar characteristics. On passing through the wake from the outside, the mean velocity drops slowly at first and then more rapidly until a minimum value is reached at the centre of the wake. Each curve of maximum velocity rises to a pronounced peak which, as will be shown later, is probably the outer boundary of the vortex street, and then falls as the centre of the wake is approached. The difference between the maximum and minimum velocities is small at some distance outside the wake but rapidly increases as the vortex street is approached. At the centre of the wake the velocity fluctuations are large, especially near the plate (see $\alpha = 90°$, $x = 5b$).

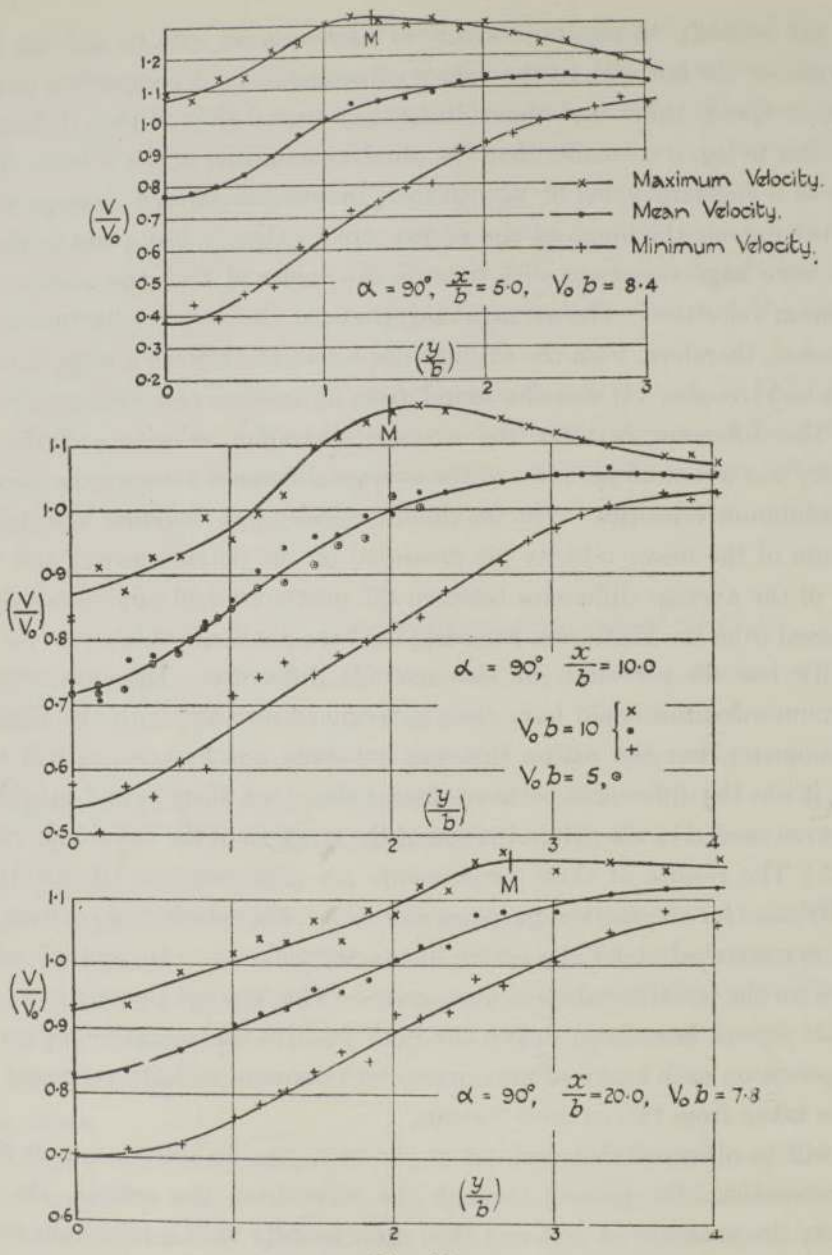

FIG. 10.

§ 8. *Vorticity in the Wake.*

(8.1.) It can easily be shown that the amplitude of the velocity fluctuations ($V_{max.} - V_{min.}$) at a point situated outside and at a distance y from the centre of a vortex street of infinite length is equal to

$$\frac{\kappa}{a}\left[\frac{1}{\sinh\frac{2\pi(y-h/2)}{a}}+\frac{1}{\sinh\frac{2\pi(y+h/2)}{a}}\right],$$

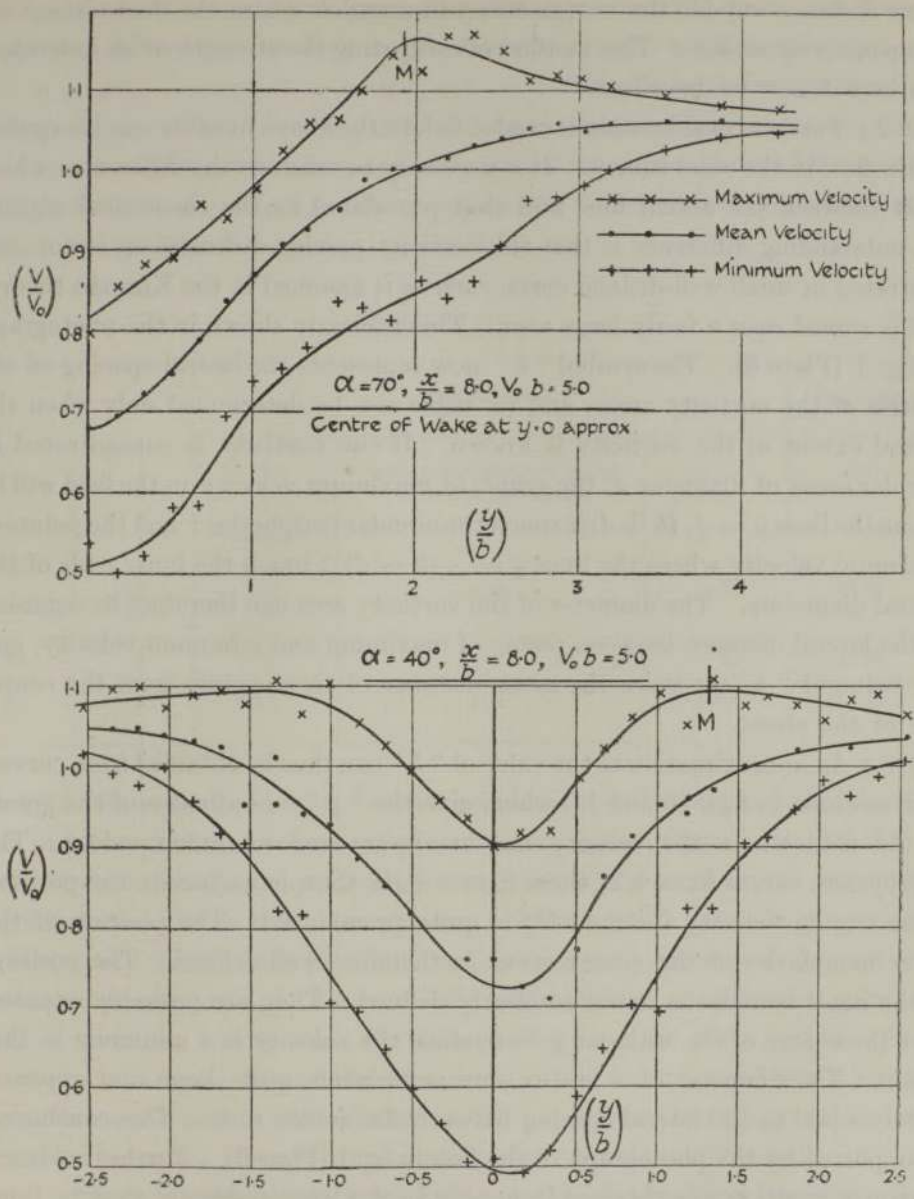

FIG. 11.

where κ is the strength of each individual vortex, and "a" and "h" are the longitudinal and lateral spacings respectively of the vortices. It follows then that when the values of "a" and "h" are known, the strength of the individual vortices can be determined from measurements of the amplitude of the velocity fluctuations outside the wake. Further, the outstanding advantage of this method of estimation is that the values of $(V_{max.} - V_{min.})$ can be measured at

some distance outside the vortex street in a region where the fluctuations are comparatively steady. This method of estimating the strength of an individual vortex will now be described.

(8.2.) Further consideration is needed before the above formula can be applied to the flow in the wind tunnel. It is necessary to examine the differences which exist between the actual flow and that postulated in the theoretical régime. An outstanding difference is that the vorticity passing downstream is not concentrated in small well-defined cores, such as is assumed in the Kármán theory, but is spread over a fairly large area. This is clearly shown in the photograph of fig. 1 (Plate 6). The symbol "h" now represents the lateral spacing of the centres of the vorticity areas, and its value can be determined only when the lateral extent of the vorticity is known. If the vorticity is concentrated in circular areas of diameter d, the points of maximum velocity in the field will be where the lines $y = \pm (h + d)/2$ touch the circular peripheries ; and the points of minimum velocity where the lines $y = \pm(h - d)/2$ touch the inner ends of the lateral diameters. The diameter of the vorticity area can therefore be regarded as the lateral distance between points of maximum and minimum velocity, and the value of "h" as twice the mean distance of these points from the centre line of the street.

(8.3.) An approximation to the value of "h" can thus be obtained from curves, such as those in figs. 10 and 11, which give the "y" co-ordinates of the points in the field where the velocity has maximum and minimum values. The appropriate curves in each of these figures show that, in each case, the position of maximum velocity (marked M) is quite pronounced. The position of the outer boundaries of the vortex street is therefore well-defined. The position of the inner boundaries is not so clearly defined. They are probably situated near the centre of the wake at $y = 0$, since the velocity is a minimum in this region. The diameter of a vortex core is therefore quite large and approximately equal to the lateral spacing between the vortex rows. This conclusion is supported by the photograph of the flow in fig. 1 (Plate 6). Further evidence worthy of mention was obtained from a study of a large number of records, from which it appeared that the velocity fluctuations over the region within the estimated outer boundaries of the vortex street were much more irregular in both frequency and amplitude, than those taken outside.

The values of "h" estimated from the curves of figs. 10 and 11 are given in Table VIII. Included in the table are the theoretical values obtained when the experimental values of "a" are substituted in Kármán's stability relation $h = 0{\cdot}281a$. The wind-tunnel values of (h/b) at $\alpha = 90°$ indicate an appreciable

opening-out of the wake with increasing distance from the plate. A direct comparison shows that, at each angle of incidence, the wind-tunnel value of "h" is greater—except at $\alpha = 90°$, $x/b = 5$—than that estimated by the Kármán theory. This may be partly due to the impossibility of ascertaining from the curves of figs. 10 and 11, any extension of the vortices beyond the centre line ($y = 0$). At the same time there appears to be definite evidence that the vortices do not flow downstream in parallel rows.

Table VIII.

$\alpha°$	(x/b)	Wind-tunnel.			Kármán.
		(h/b)	(y/b) co-ordinate of point in outer boundary.	(a/b)	(h/b)
90	5 10 20	1·30 2·0 2·75	1·3 2·0 2·75	5·25	1·48
70	8	1·9	1·9	4·85	1·36
40	8	1·3	1·3	3·55	1·00

(8.4.) Another point which needs investigation is the extent to which the formula given in § 8.1, which has been derived on the assumption that the length of the vortex street is infinite, is applicable to the street in the wind-tunnel where the length is finite. To do this a formula was obtained which gave the magnitude of the velocity fluctuations for the actual number and spacing of the vortices in the tunnel, when the plate was at 90°. The number of individual vortices taken in each row was 5, since the distance between the plate and the after end of the tunnel was about $5 \cdot 4a$ at $\alpha = 90°$. The formula used was a simple summation series and is not included in the paper because of its cumbersome nature. The vortex strength estimated by this formula is compared with that calculated for an infinite street, having the same longitudinal and lateral spacing of vortices, in Table IX. The two methods give results which are in close agreement (within 4 per cent.). The agreement will, of course, become closer as the angle of incidence decreases and the value of "a" becomes smaller. Since only an approximate value of the vortex strength is needed it was considered that it would be sufficiently accurate to use, in all cases, the simpler formula, *i.e.*, that for the infinite street.

(8.5.) The effect of the tunnel walls on the value of $(V_{max.} - V_{min.})$ was

Table IX.

$\alpha°$	(x/b)	(y/b)	$(V_{max.}-V_{min.})/V_0$.	Series I. Kármán.			Series II. Wind-tunnel.			K/V_0^2 from Table VI.	$(\kappa f/K)$	
				(h/b)	$\kappa/V_0 b$.	$\kappa f/V_0^2$.	(h/b)	$\kappa/V_0 b$.	$\kappa f/V_0^2$.		Series I (mean).	Series II (mean).
90	10	3·0	0·151	1·475	5·1 (4·9)*	0·74 (0·72)*	2·0	3·9 (3·9)*	0·57 (0·57)*	1·10	0·65 (0·63)*	0·51 (0·49)*
		3·8	0·055	1·475	4·8 (4·5)*	0·70 (0·66)*	2·0	3·8 (3·5)*	0·55 (0·51)*			
70	8	3·0	0·128	1·365	5·3	0·83	1·9	4·1	0·64	1·00	0·82	0·63
		4·0	0·034	1·365	5·2	0·81	1·9	4·0	0·62			
40	8	1·8	0·146	1·000	2·2	0·51	1·3	1·8	0·41	0·95	0·64	0·51
		2·5	0·057	1·000	3·0	0·69	1·3	2·4	0·55			

* Finite street.

investigated and found to be negligible. This result is to be expected since the lateral spacing between the vortex rows is small compared with the width of the tunnel, so that the rows of positive and negative vorticity in each image neutralise each other in so far as their effect at a distance is concerned.

(8.6.) Estimations of the average strength of the individual vortices at some distance behind the plate (about $9b$), when $\alpha = 90°$, $70°$ and $40°$ are given in Table IX. To show the effect on $(\kappa/V_0 b)$ of a change in the value of "h," two series of results are given. In the first, the Kármán values of "h" have been taken, and in the second, the wind-tunnel values. In all cases, the calculations were made for two values of $(V_{max.} - V_{min.})$ measured in the comparatively steady region outside the vortex street. The values of the vortex strength are expressed in non-dimensional units by dividing by the product $(V_0 b)$.

The results given in Table IX show that :—

(a) At $\alpha = 90°$, the value of $(\kappa/V_0 b)$ calculated for the infinite and finite streets are in close agreement.

(b) At $\alpha = 90°$ and $\alpha = 70°$ the values of $(\kappa/V_0 b)$ calculated for the two values of $(V_{max.} - V_{min.})/V_0$ at the same value of (h/b) are in close agreement. This is, however, not the case at $\alpha = 40°$.

(c) At the same incidence, and for the same values of $(V_{max.} - V_{min.})/V_0$, the values of $(\kappa/V_0 b)$ are smaller in Series II (wind-tunnel) than in Series I (Kármán), (about 20 per cent.).

It may be concluded that the above method of calculation gives a reasonably good estimate of the average strength of the individual vortices, even although some uncertainty probably arises from the difficulty of estimating the exact value of "h." It is for this reason that the calculations were made both for the Kármán and experimental values of "h."

(8.7.) The most interesting results in Table IX are those which give the values of $(\kappa f/K)$, that is, the ratio of the rate at which vorticity is carried downstream in the form of well-defined vortices to the rate at which it is generated at the edge of the plate. There appears to be no systematic variation of $(\kappa f/K)$ with α, so that for the purpose of discussion it is sufficient to take the mean values in each column. These are 0·70 (Series I) and 0·55 (Series II). It follows, then, that not all the vorticity which leaves the edge travels downstream in the form of individual vortices. Of the remainder, undoubtedly a part is dissipated immediately behind the plate, by a mixture of the positive and negative vorticity from the two edges, and the rest possibly passes downstream as "unattached" vortices, which are too small to affect appreciably the measured velocity fluctuations outside the wake. It has also to be borne in mind, that

even the large vortices themselves tend to break up and lose their individuality, as the distance behind the plate increases. This is clearly shown by the velocity records (Nos. 3 to 8) given in fig. 6 (Plate 7) and the photograph of fig. 1 (Plate 6). The general conclusion that can be drawn is that at a distance of $9b$ (approximately) behind the plate about 60 per cent. of the vorticity leaving the edge is passing downstream in the form of large vortices having a definite individuality; and whilst no positive evidence is available, it is highly probable that an appreciable dissipation of vorticity occurs at the back of the plate.

§ 9. *A Note on Kármán's Vortex Theory.*

(9.1.) Kármán has given a formula for the resistance of a flat plate moving normal to the stream, in terms of the dimensions of the vortex system behind the plate. This formula, given in the symbols of the paper, is

$$k_D = 0{\cdot}281\ a/b\ [2{\cdot}83\ (1 - V_3/V_0) - 1{\cdot}12\ (1 - V_3/V_0)^2].$$

If the second term be neglected the formula reduces to the approximate form $k_D = 0{\cdot}795\ .\ a/b\ (1 - V_3/V_0)$, or $k_D = 0{\cdot}281\ (\kappa/V_0 b)$ (see § 9.2). The drag is then proportional to the strength of the individual vortices. A comparison between the measured values of drag and those obtained from these two formulæ, when the wind-tunnel values of (a/b) and (V_3/V_0) are substituted, is given in Table X. Although the theory relates to a plate at 90° incidence, additional calculations have been made for values of α below 90°; this appears to be legitimate since earlier work (§§ 4.7 and 5.2) has shown that the flow pattern at some distance behind the inclined plate closely resembles that behind a plate of width $(b \sin \alpha)$ mounted normal to the wind.

Table X.

$\alpha°$	Wind-tunnel.		k_D.	k_D.		Col. B / Col. A	Col. C / Col. A
	(a/b)	(V_3/V_0)	k_D. (A)	Kármán's formula. (B)	Kármán's approx. formula. (C)		
90	5·25	0·765	1·065	0·895	0·980	0·84	0·92
70	4·85	0·755	0·975	0·855	0·945	0·88	0·97
60	4·44	0·760	0·850	0·770	0·850	0·91	1·00
50	4·08	0·790	0·690	0·625	0·680	0·91	0·99
40	3·55	0·815	0·505	0·485	0·520	0·96	1·03
30	2·76	0·840	0·325	0·335	0·350	1·03	1·08

The last two columns of Table X show that fair agreement exists between the wind-tunnel and the Kármán values of k_D; but a closer agreement is obtained when the approximate formula is used.

(9.2.) Another theoretical relationship given by Kármán is :—

$$(\kappa/V_0 b) = 2\sqrt{2}\,(a/b)\,(1 - V_3/V_0).$$

Table XI gives the Kármán values of $(\kappa/V_0 b)$ when the experimental values of (a/b) and (V_3/V_0) are substituted in this formula, and also the wind-tunnel values.

Table XI.

$\alpha°$	Wind-tunnel.			Kármán.
	(a/b)	(V_3/V_0)	$(\kappa/V_0 b)$	$(\kappa/V_0 b)$
90	5·25	0·765	3·9	3·50
70	4·85	0·755	4·0	3·35
40	3·55	0·815	2·1	1·85

The agreement between the wind-tunnel ($x/b = 9{\cdot}0$ approx.) and the Kármán values of $(\kappa/V_0 b)$ is reasonably close. It has already been shown in Table VIII that, in general, the wind-tunnel values of "h" are higher than those of theory.

(9.3.) It should be recorded that the Kármán values of (a/b) and (fb/V_0) measured in water, with the plate normal to the general stream, are in close agreement with those measured in the present experiments. The actual values are 5·50 and 0·145 (Kármán), and 5·25 and 0·146 (N.P.L.).

§ 10. *Summary.*

The periodic flow behind an infinitely long flat plate inclined in an air stream is examined by means of a heated hot wire used in conjunction with an Einthoven galvanometer.

The vortices generated at each edge pass downstream with a frequency which increases as the inclination of the plate decreases. The frequency is proportional to the wind speed, at a constant inclination.

The longitudinal spacing of the vortices decreases as the inclination of the plate decreases. The vortices pass downstream at a speed which increases as the inclination decreases.

Vorticity is shed from the two edges of the plate at the same rate. This rate falls slowly as the inclination is decreased from 90°.

There is a lateral opening-out of the vortex street with the passage downstream.

Only a part of the vorticity leaving the plate travels downstream in the form of vortices having a definite individuality.

Kármán's formula for the resistance of a flat plate, given in terms of the dimensions of the vortex system behind the plate, gives results in fair agreement with those measured directly. The Kirchhoff-Rayleigh theory considerably underestimates the force acting on the plate.

In conclusion, the writers desire to acknowledge their great indebtedness to Dr. H. Lamb, F.R.S., for valuable criticisms and suggestions made during the preparation of the paper, and also to Dr. S. B. Young and Mr. S. Ward, of the Admiralty Research Laboratory (Teddington), for the loan of the Einthoven galvanometer.

[*Added, August* 16, 1927.—Since the paper was communicated, Mr. H. Glauert, of the Royal Aircraft Establishment, has pointed out that the wind-tunnel values of k_D given in Table X should be corrected for the interference of the wind-tunnel, because they are compared with Kármán values of k_D for a plate in a free stream. He has also shown from theoretical considerations that the tunnel effect may be important when the plate is normal to the stream. To determine the magnitude of this effect for the 6-inch plate used in the above experiments, additional experiments have been made, in the manner described in § (3.2), to measure the drag of flat plates, of breadths 2, 4 and 8 inches respectively, set normal to the air stream in a 7-foot tunnel. From these measurements, and that previously obtained for the 6-inch plate, an approximate value of the drag coefficient (k_D) for a normal flat plate in a free stream has been obtained. The results are given below, and show that the observed drag coefficient (k_D) of 1·065 (6-inch plate) would be reduced to 0·92 approximately in the absence of the constraint of the tunnel walls. It was also estimated that the probable reduction in k_D for the plate at $\alpha = 30°$ would be 8 per cent. The wind-tunnel values of k_D in Table X should therefore be reduced by amounts varying from 13·5 per cent. at $\alpha = 90°$ to 8 per cent. at $\alpha = 30°$. These corrections bring the experimental results into much closer agreement with the Kármán values of k_D given in column B, and the general agreement with theory is satisfactory.

Breadth of Plate in inches.	$\left(\frac{\text{Breadth of Tunnel}}{\text{Breadth of Plate}}\right)$	Drag Coefficient.* k_D.
8	10·5	1·072
6	14·0	1·065
4	21·0	1·025
2	42·0	0·964
—	∞	0·920 (estimated)

* These values were obtained by dividing the measured drag per unit length of the plate by $(\rho b V_0^2)$, where V_0 is the velocity of the undisturbed wind.

It will be apparent from the context that the comparison of

$$\frac{V_1^2 \text{ (wind-tunnel)}}{V_0^2 \text{ (Kirchhoff-Rayleigh Theory)}} \quad \text{with} \quad \frac{k_N \text{ (wind-tunnel)}}{k_N \text{ (Kirchhoff-Rayleigh Theory)}}$$

referred to at the end of § (3.5) still stands, and that the experimental values of k_N should not be corrected for the constraint of the tunnel.]

The Photosynthesis of Naturally Occurring Compounds. I.—*The Action of Ultra-Violet Light on Carbonic Acid.*

By E. C. C. Baly, F.R.S., J. B. Davies, M. R. Johnson, and H. Shanassy, Liverpool University.

(Received July 28, 1927.)

Introduction.

In a preliminary paper one of us, in conjunction with Prof. Heilbron and Prof. Barker,* described some observations on the action of ultra-violet light on pure aqueous solutions of carbonic acid. It was found that traces of formaldehyde were present in these solutions after insolation, provided that a stream of the gas were passed through the water during the exposure to the light. These results differed from those which had previously been recorded by Moore and Webster,† who had stated that the presence of a catalyst such as colloidal ferric or uranium hydroxide was necessary.

The observation by Moore and Webster that formaldehyde in aqueous solution

* 'Trans. Chem. Soc.,' vol. 119, p. 1025 (1921).

† 'Roy. Soc. Proc.,' B, vol. 87, p. 163 (1914), and vol. 90, p. 168 (1918).